Self-Organization and Pattern Formation of Janus Particles in Two Dimensions by Computer Simulations

Alexandros G. Vanakaras*

Department of Materials Science, University of Patras, Patras 26504, Greece

Received July 27, 2005. In Final Form: October 20, 2005

The phase behavior and associated pattern formation of two-dimensional systems of hard disks decorated with amphiphilic coronae (Janus disks) are studied by means of Monte Carlo computer simulations. A primitive interaction potential that captures the essential interparticle interactions is introduced. Despite its simplicity, the system exhibits a very rich phase polymorphism. Apart from the isotropic phase and depending upon the coronal thickness, the simulated systems self-organize in a number of two-dimensional mesophases of various symmetries exhibiting a variety of novel patterns. The results of these simulations suggest that 2D Janus particles are promising candidates for bottom−up design of precise two-dimensional templates.

Introduction

Understanding the principles that govern the bottom−up approach to molecular self-assembly and self-organization is a scientific challenge in its own right and integral to successful fabrication of self-organized systems with desirable functionality via molecular engineering.[1−3] Thermotropic and lyotropic liquid crystals,[4] Langmuir monolayers,[5] phase-separated polymers,[6] dendrimers[7] and colloidal crystals[8] are just a few of the numerous systems whose technological applications are based on their intrinsic property to self-organize under certain thermodynamic conditions. One of the most striking signatures of self-organization is spontaneous pattern formation. Depending upon the molecular properties and thermodynamic conditions, self-organization may involve molecular self-assembly. In the later case, self-organization drives and is driven by spontaneous formation of supramolecular entities that remain associated by non- or weakly covalent interactions. The self-assembled aggregates may consist of a few, just two or three molecules, or several hundreds or thousands of molecules, thereby forming structures on length scales of nano- or micrometers.[9] Furthermore, the physicochemical properties of the self-assembled aggregates are in general rather different from those of their constituent parts and usually depend critically upon the size, shape, and polydispersity of the assemblies.[10,11] This in turn gives a wide range of options to create, in a controllable fashion, periodic macrostructures with tailored functionality.

The so-called core−shell or core−corona particles represent a broad class of systems that have been intensively investigated during the past few years. Typical systems exhibiting such a composite architecture include metal or glass nanoparticles,[12] block copolymer micelles,[13] and globular dendrimers.[14] One of the unique characteristics of such systems is the coexistence, in a single structure, of three distinct topological regions: the internal core, the coronal region, and an external surface. The well-defined architecture, together with the possibility of chemical modification of all three distinct regions, offers a multitude of molecular designs for particles with unique properties that are amenable to self-assembly. Recently, Malescio and Pellicane showed by means of computer simulations that 2D systems with core−corona architecture interacting only via repulsive interactions may spontaneously form stripe patterns because of two repulsive length scales characterizing core and corona properties.[15] Using a rather different approach, Zhang and Glotzer[16] suggested that nanoparticles whose surfaces are patterned with "sticky patches" might group together into well-defined shapes. Their computer simulation results show that it is possible to achieve rather exotic and thermodynamically stable structures by properly designing the nanoparticle surface. These two computer simulation studies, utilizing highly idealized molecular interactions, reveal that either submolecular partioning into chemically distinct regions or modification of well-defined structures with selectively interacting sites influences dramatically the self-organization behavior of the systems.

In this paper, we present computer simulation results for a special class of core−shell systems bearing the so-called Janus property (one-half of the outer shell is hydrophilic and the other is hydrophobic).[17] There are several examples of supermolecules of dendritic topology, either mesogenic[18] or not,[19] having the dendritic periphery separated into hydrophobic and hydrophilic

* To whom correspondence should be addressed. E-mail: vanakara@upatras.gr.

(1) Lehn, J.-M. *Proc. Natl. Acad. Sci. U.S.A.* **2002**, *99*, 4763.
(2) Whitesides, G. M.; Boncheva, M. *Proc. Natl. Acad. Sci. U.S.A.* **2002**, *99*, 4769.
(3) Tschierske, C. *Curr. Opin. Colloid Interface Sci.* **2002**, *7*, 69.
(4) *Handbook of Liquid Crystals*; Demus, D., Goodby, J., Gray, G. W., Spiess, H.-W., Vill, V., Eds.; Wiley-VCH: Weinheim, Germany, 1998; Vol. 1−3.
(5) Petty, M. C. *Langmuir−Blodgett Films: An Introduction*; Cambridge University Press: Cambridge, U.K., 1996.
(6) Stupp, S. I.; LeBonheur, V.; Walker, K.; Li, L. S.; Huggins, K. E.; Kesse, M.; Amstutz, A. *Science* **1997**, *276*, 384.
(7) (a) Hudson, S. D.; Jung, H. T.; Percec, V.; Cho, W. D.; Johansson, G.; Ungar, G.; Balagurusamy, V. S. K. *Science* **1997**, *278*, 5337. (b) Tomalia, D. A. *Mater. Today* **2005**, *8*, 34.
(8) Manna, L.; Milliron, D. J.; Meisel, A.; Scher, E. C.; Alivisatos, A. P. *Nat. Mater.* **2003**, *2*, 382.
(9) Whitesides, G. M.; Grybowski, B. *Science* **2002**, *295*, 2418.
(10) Milliron, D. J.; Hughes, S. M.; Cui, Y.; Manna, L.; Li, J. B.; Wang, L. W.; Alivisatos, A. P. *Nature* **2004**, *430*, 190.
(11) Burda, C.; Chen, X.; Narayanan, R.; El-Sayed, M. A. *Chem. Rev.* **2005**, *105*, 1025.
(12) (a) Green, M. *Small* **2005**, *1*, 684. (b) Ow, H.; Larson, D. R.; Srivastava, M.; Baird, B. A.; Webb, W. W.; Wiesner, U. *Nano Lett.* **2005**, *5*, 113.
(13) (a) Riess, G. *Prog. Pol. Sci.* **2003**, *28*, 1107. (b) Kang, N.; Perron, M. E.; Prudhomme, R. E.; Zhang, Y. B.; Gaucher, G.; Leroux, J. C. *Nano Lett.* **2005**, *5*, 315. (c) Katsampas, I.; Tsitsilianis, C. *Macromolecules* **2005**, *38*, 1307.
(14) (a) Zeng, F.; Zimmerman, S. C. *Chem. Rev.* **1997**, *97*, 1681. (b) Bosman, A. W.; Janssen, H. M.; Meijer, E. W. *Chem. Rev.* **1999**, *99*, 1665. (c) Grayson, S. M.; Frechet, J. M. *J. Chem. Rev.* **2001**, *101*, 3819.
(15) (a) Malescio, G.; Pellicane, G. *Nat. Mater.* **2003**, *2*, 97. (b) Malescio, G.; Pellicane, G. *Phys. Rev. E* **2004**, *70*, 021202.
(16) Zhang, Z.-L.; Glotzer, S. C. *Nano Lett.* **2004**, *4*, 1407.
(17) (a) de Gennes, P.-G. (Nobel Lecture) *Angew. Chem., Int. Ed. Engl.* **1992**, *31*, 842. (b) de Gennes, P.-G. *Croat. Chem. Acta* **1998**, *71*, 833.

10.1021/la052036g CCC: $33.50
Published on Web 12/03/2005

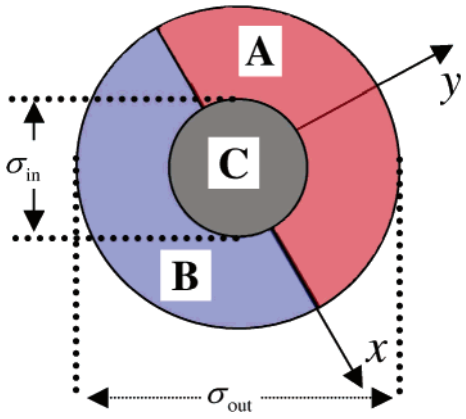

Figure 1. Model disklike Janus particle used in the simulations. It consists of the internal hard core (C) of diameter σ_{in} and a soft corona with outer diameter σ_{out} divided into two sections (A and B) of opposite philicity.

domains. Similarly, however, on the basis of triblock copolymers, nanospheres with amphiphilic coronal chains have been synthesized.[20,21] Furthermore, Schluter and co-workers have reported[22] the synthesis of rodlike molecules with two different half-coronas based on polydendrons with opposite philicities. Going beyond molecular systems, Whitesides' group has succeeded in making spherical nanoparticles that are coated with a gold film on only one hemisphere, thereby permitting the synthesis of two-faced (Janus) particles.[23] In addition, Paunov and Cayre were able to prepare asymmetrically coated colloidal particles using a gel-trapping technique.[24] Very recently, self-assembly has been used to prepare multicomponent polymeric microspheres of arbitrary internal symmetries,[25] and new strategies for fabrication of asymmetrically functionalized Janus microspheres have been reported.[26]

The aim of the computer simulations presented herein is to clarify the combined effect of amphiphilicity and coronal thickness of model Janus particles on their equilibrium, two-dimensional self-organization characteristics and the nature of their pattern formation. To do this, a minimal two-dimensional molecular model is introduced. Despite its simplicity, the self-organization behavior and rich accompanying pattern formation of such systems are anticipated to elucidate the role of the Janus property on the self-organization of such systems and to provide design rules for nanoparticles or molecules to be utilized for the creation of templated surface structures.

Molecular Model and Computational Details

A highly idealized representation of a disklike Janus particle in two dimensions is sketched in Figure 1. The model particle consists of two homocentric disks with diameters $\sigma_{in} \leq \sigma_{out}$. The internal disk, denoted by C, is assumed to represent the hard core of the Janus particle, while the soft coronal region around the hard core is bounded by the perimeter of the outer large disk. To introduce the different faces of the Janus particle, the coronal part is furthermore subdivided, by an arbitrary diameter, into two geometrically identical regions, A and B, distinguished by different colors in Figure 1. These coronal parts represent the submolecular regions of opposite philicity, i.e., the two different half-sectors of the Janus particle. Such a 2D system could be obtained, for example, from amphiphilic disklike molecules adsorbed onto a surface, with core−substrate interactions rendering the disk coplanar with the surface.[27]

Because of the different properties of the two sectors, the cylindrical symmetry of the particle is broken, imparting polarity to the disk. An orthogonal molecular frame, rigidly attached to the center of the particle, is introduced, with the *x* axis lying along the diameter that separates the two sectors and the *y* axis passing pointing toward the A region. The interparticle potential $u(\mathbf{r}_{ij},\omega_{ij})$ between a pair of particles *i* and *j* depends upon the center−center interparticle vector, $\mathbf{r}_{ij}$, and on their relative orientation ω_{ij}. A double-valued overlap function $F_{ab}(\mathbf{r}_{ij},\omega_{ij})$ is introduced to formulate the interparticle potential. This function is 1 if any of the submolecular parts *a* (=A, B, and C) of particle *i* overlap with any part *b* (=A, B, and C) of the particle *j* and is 0 otherwise. The interparticle potential can be expressed in terms of the overlap function $F_{ab}(\mathbf{r}_{ij},\omega_{ij})$ as follows $u(\mathbf{r}_{ij},\omega_{ij}) = \sum_{ab} u_{ab}F_{ab}(\mathbf{r}_{ij},\omega_{ij})$, with u_{ab} playing the role of "molecular" parameters that control the strength of the interparticle interaction among the submolecular parts. There are six different interaction parameters u_{ab} for the specific primitive model of the Janus particle. In general u_{ab} is a function of both interparticle vector $\mathbf{r}_{ij}$ and of the relative orientation ω_{ij}. In the present calculations and to keep the intermolecular potential as simple as possible, retaining at the same time the core-amphiphilic-shell nature of the Janus particle, we assume that $u_{AA} = u_{BB} = 0$ and $u_{AB} = u_{AC} = u_{BC} = u_{CC} = \infty$. With this parametrization, a pair of particles experiences infinite repulsion upon overlap (i) of their coronal sectors of opposite philicity or (ii) of the internal core with the amphiphilic coronae. Moreover, this parametrization implies that coronal sectors of the same philicity may overlap without any energetic loss or gain.

The dimensionless molecular parameter $\chi \equiv (\sigma_{out} - \sigma_{in})/\sigma_{out}$ is introduced to quantify the thickness of the soft amphiphilic corona. Because $\sigma_{in} \leq \sigma_{out}$, the reduced thickness parameter χ assumes values in the interval $0 \leq \chi \leq 1$. When $\chi = 0$, the soft amphiphilic corona has 0 thickness and the particle is simply a hard disk with diameter $\sigma_{in} = \sigma_{out}$. At the other extreme, when $\chi = 1$, the internal hard core is absent and the particle consists of just two soft hemidisks of opposite philicity. It is clear that the interactions are characterized by two molecular lengths: (i) the distance, $\sigma_{max} \equiv \sigma_{out}$, beyond which any two particles do not interact and (ii) the distance of the shortest approach for any pair of particles, $\sigma_{min} \equiv (\sigma_{out} + \sigma_{in})/2 = (1 - \chi/2)\sigma_{out}$. In the present calculations, the distance, σ_{min}, is used as the length unit.

To simulate the phase behavior of such systems, we have performed standard constant pressure (tension) Monte Carlo simulations.[28,29] *N* particles are initially positioned in a rectangular box at low density, and the system is left to equilibrate at a given low pressure. Once the resultant phase is isotropic, the system is gradually compressed with small pressure jumps. The final equilibrated configuration of a given pressure is used as the initial configuration for the next higher pressure simulation run. Each simulation involves approximately 10^5 Monte Carlo (MC) cycles for equilibration, and statistics is obtained during the next 10^6 MC cycles. On a MC cycle, each of the *N* particles is attempted to translate and reorient one time on average and a box-surface change is attempted. To avoid the development of internal stresses, especially in the high-pressure-

(18) (a) Saez, A. M.; Googby, J. W. *J. Mater. Chem.* **2005**, *15*, 26. (b) Saez, A. M.; Googby, J. W. *Chem.—Eur. J* **2003**, *9*, 4869.
(19) (a) Guillon, D.; Nierengarten, J.-F.; Gallani, J. L.; Eckert, J. F.; Rio, Y.; Carreon, M. D.; Dardel, B.; Deschenaux, R. *Macromol. Symp.* **2003**, *192*, 63. (b) Nierengarten, J.-F.; Eckert, J.-F.; Rio, Y.; del Pilar Carreon, M.; Gallani, J.-L.; Guillon, D. *J. Am. Chem. Soc.* **2001**, *123*, 9743. (c) Ropponen, J.; Nummelin, S.; Rissane, K. *Org. Lett.* **2004**, *6*, 2495.
(20) Hoppenbrouwers, E.; Li, Z.; Liu, G. *Macromolecules* **2003**, *36*, 876.
(21) Erhardt, R.; Zhang, M.; Boker, A.; Zettl, H.; Abetz, C.; Frederik, P.; Krausch, G.; Abetz, V.; Muller, A. H. E. *J. Am. Chem. Soc.* **2003**, *125*, 3260.
(22) (a) Bo, Z. S.; Rabe, J. P.; Schluter, A. D. *Angew. Chem. Int. Ed.* **1999**, *38*, 2370. (b) Schluter, A. D.; Rabe, J. P. *Angew. Chem. Int. Ed.* **2000**, *39*, 864.
(23) Love, J. C.; Gates, B. D.; Wolfe, D. B.; Paul, K. E.; Whitesides, G. M. *Nano Lett.* **2002**, *2*, 891.
(24) Paunov, V. N.; Cayre, O. J. *Adv. Mater.* **2004**, *16*, 788.
(25) Fialkowski, M.; Bitner, A.; Grzybowski, B. A. *Nat. Mater.* **2005**, *4*, 93.
(26) Li, Z.; Lee, D.; Rubner, M. F.; Cohen, R. E. *Macromolecules* **2005**, *38*, 7876.
(27) (a) Loi, S.; Wiesler, U.-M.; Butt, H.-J.; Mullen, K. *Macromolecules* **2001**, *34*, 3661. (b) Loi, S.; Butt, H.-J.; Hampel, C.; Bauer, R.; Wiesler, U.-M.; Mullen, K. *Langmuir* **2002**, *18*, 2398. (c) Xia, C.; Fan, X.; Locklin, J.; Advincula, R. C.; Gies, A.; Nonidez, W. *J. Am. Chem. Soc.* **2004**, *126*, 8735.
(28) Allen, M. P.; Tildesley, D. J. *Computer Simulation of Liquids*; Clarendon Press: Oxford, U.K., 1987.
(29) Frenkel, D.; Smit, B. *Understanding Molecular Simulation: From Algorithms to Applications*; Academic Press: London, U.K., 2001.

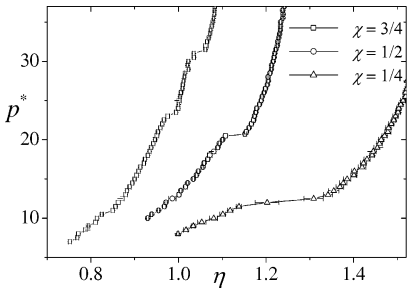

Figure 2. Plots of the calculated pressure versus packing fraction ($p^*-\eta$) equation of the state for three different systems of Janus disks with the corona reduced thickness $\chi = {}^1/_4$ (□), ${}^1/_2$ (○), and ${}^3/_4$ (△).

ordered phases, the shape of the box is allowed to change during the surface change attempts.

For the structural characterization of the simulated phases, several pair correlation functions have been calculated. The simplest is the orientationally averaged radial correlation function, $g(r)$, which gives the probability to find a pair of molecules at a distance between $r - dr/2$ and $r + dr/2$. It is defined as $g(r) = 1/2\pi r\langle 1/\rho\ \delta(r - r_{ij})\rangle_{ij}$, where r_{ij} is the center−center distance of the molecules i and j and $\rho = N/S$ is the number surface density, with S the surface area of the simulation box. Here, $\langle\cdots\rangle_{ij}$ represents the ensemble average of the bracketed function with respect to all of the molecular pairs. Orientational radial pair correlation functions are calculated in the course of the simulations. An informative set of such, distance-dependent, orientational correlation functions may be defined as $g_m(r) = \langle\delta(r_{ij} - r)\cos(m\varphi_{ij})\rangle_{ij}/\langle\delta(r_{ij} - r)\rangle_{ij}$, with $m > 1$, where $\varphi_{ij} \equiv \cos^{-1}(\mathbf{y}_i\cdot\mathbf{y}_j)$ is the angle made by the molecular y axes of the molecules i and j. In the absence of long range orientational correlations, i.e., for the orientationally disorderd isotropic phases, the functions $g_m(r)$ are expected to exhibit a significant structure only up to distances of a few molecular diameters (because of the strong orientational anisotropy of the intermolecular potential) and to decay rapidly to 0 for longer distances. In case the system exhibits either long or quasilong orientational order, the long-distance behavior of the functions $g_m(r)$ indicates the range and the symmetry elements of the orientational order.

Results and Discussion

To clarify the role of the relative thickness of the amphiphilic corona on the phase behavior and on the pattern formation, several systems with coronal thickness parameter χ in the range of 0−1 were simulated. The $p^*-\eta$ equations of the state (with $p^* = P\sigma_{min}{}^2/kT$, the dimensionless pressure (tension), and $\eta = \langle\rho\rangle(\pi\sigma_{min}{}^2/4)$, the corresponding ensemble average of the packing fraction of the system) are plotted in Figure 2 for three representative cases corresponding to thin ($\chi = {}^1/_4$), moderate ($\chi = {}^1/_2$), and thick ($\chi = {}^3/_4$) corona using respectively $N = 576$, 896, and 572 particles in the simulation box.

The system with $\chi = {}^1/_4$ is the one with the richest phase polymorphism among the studied systems. The phase-transition pressures are easily identified from the discontinuities in the equation of the state plot of Figure 2. A first insight into the structural differences between the various phases is obtained by simple visual inspection of the representative snapshots shown in parts a−d of Figure 3. Particles belonging to instantaneously formed percolation clusters, e.g., clusters of "linked" particles with overlapping coronal regions, are depicted with different colors depending upon the cluster size (the color code is described in the caption of Figure 3). At low pressures, $p^* < 12$, the system with $\chi = {}^1/_4$ behaves as a two-dimensional isotropic fluid. Snapshots in this range of pressures suggest that the system does not exhibit any long-range positional or orientational correlations.

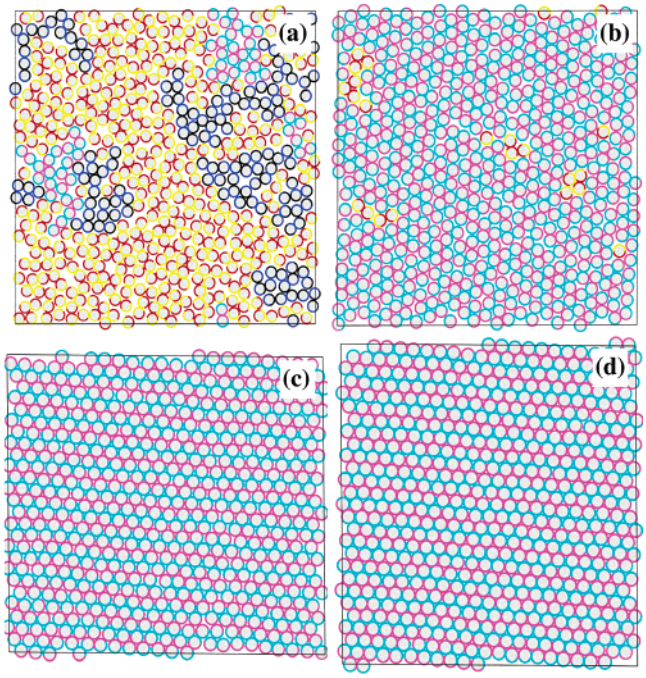

Figure 3. Typical snapshots at (a) $p^* = 7$, (b) 15, (c) 27, and (d) 36 of the four different phases exhibited by the $\chi = {}^1/_4$ system. A color code for the coronal regions of opposite philicity is used to convey molecular percolation clusters of different sizes: (red/yellow) for particles participating in clusters composed of less than 5 disks, (black/blue) clusters composed of 5−49 particles, and (magenta/light blue) clusters with more than 50 particles. The same color code is used for all of the simulation snapshots presented in subsequent figures.

This is confirmed by the plots of the radial correlation functions, given in parts a and e of Figure 4, from which it is clear that both positional and orientational correlations decay rapidly to 0 with the distance. However, the short-distance structure of the radial correlation function, $g(r)$, indicates significantly different short-distance correlations from a conventional isotropic hard-disk system. Here, as a result of the two characteristic molecular-length scales, the first peak that appears in conventional hard-disk systems is split into a pair of peaks corresponding to the two interparticle separations σ_{min} and σ_{max}, respectively.

From the equation of the state, it is clear that, at $p^* \approx 12$, the $\chi = {}^1/_4$ system exhibits a first-order phase transition from the isotropic to a positionally ordered phase (as indicated by the snapshot of Figure 3b) that remains stable up to $p^* \approx 23$. The pair distribution function $g(r)$, shown in Figure 4b, illustrates clearly the appearance of relatively long-range positional order. The two characteristic molecular lengths explain, in the same way as for the disordered low-pressure phase, the splitting of first peak in $g(r)$. The higher intensity peak, associated with the larger molecular length, σ_{max}, reveals that this length dominates the distance dependence of the molecular correlations in both phases. As in the disordered phase, the particles rotate almost freely about the axis normal to their plane. However, a closer look at the orientational radial pair correlation functions $g_6(r)$, shown in Figure 4f, reveals that the positionally ordered phase has developed long-range orientational correlations. The fact that all lower than the sixth-order orientational correlations vanish at long distances suggests that the system possesses a 6-fold symmetry axis.

At $p^* \approx 23$, the $\chi = {}^1/_4$ system exhibits a second phase transition. Independent simulation runs of both compressions and expansions for systems of various sizes suggest that this transition is of first order and is accompanied by a smaller density jump with respect

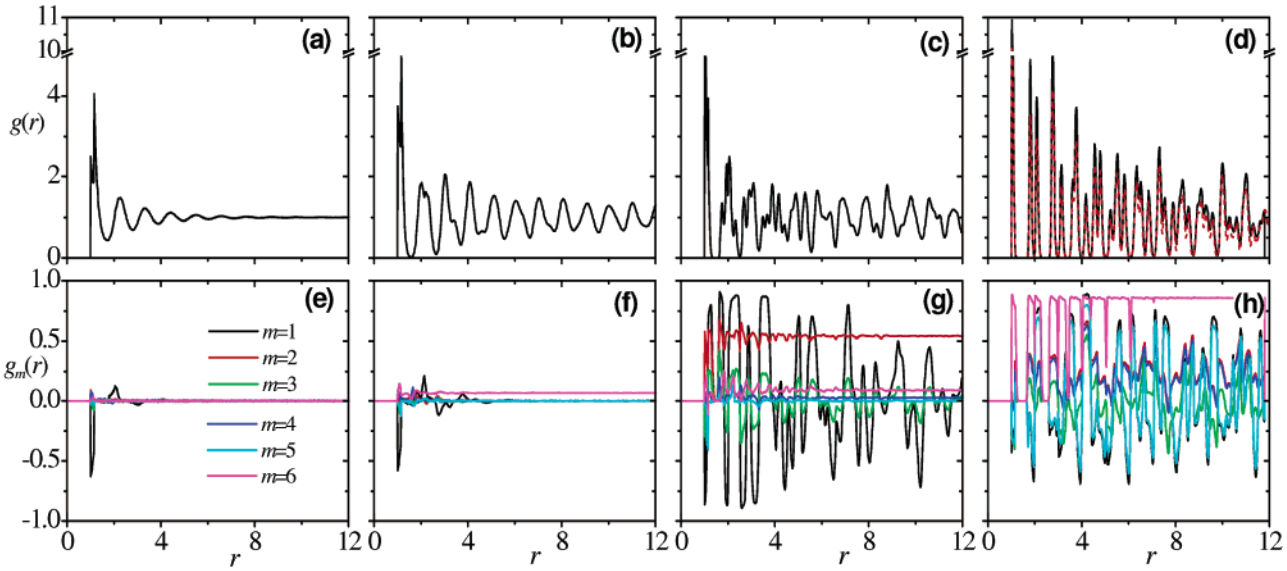

Figure 4. Calculated radial correlation functions (a−d) and orientational correlation functions (e−h) at four different pressures (see the caption of Figure 3) corresponding to the four different phases exhibited by the $\chi = {}^1/_4$ system.

to the first phase transition. Inspection of the snapshots of the new phase (Figure 3c shows one at $p^* = 27$) makes it clear that the positional order of the new phase is somewhat higher than the previous one, but the two phases differ clearly in their long-range orientational order. Moreover, the new phase is clearly accompanied by spontaneous pattern formation, indicating the development of strong orientation−position correlations. This phase has apparent analogies with lamellar phases, with the molecules forming well-defined stripes. The particles in each stripe are preferentially oriented with their local y axes normal to the stripe and parallel to one another on average, thus assembling into the polar stripe with the polarity exhibited transversely to the stripe direction. However, the system appears overall apolar because of antiparallel stacking of successive stripes. The pair correlation functions are substantially more structured than the corresponding functions of the less ordered phase. Starting with $g(r)$, shown in Figure 4c, we observe that the relative intensity of the first two peaks is reversed. This indicates that the large characteristic molecular length, σ_{max}, does no longer dominate the short-range correlations. The height ratio of the first two peaks is about 2 in favor of the first. This suggests that, among the six first neighbors of a given particle, four of them are at a distance σ_{min} and two of them are at a distance σ_{max}, in accordance with the visual inspection of the snapshots (see Figure 3c). In this phase, therefore, adjacent particles are more likely to be found within distances that allow extended overlap between the coronal sectors of the same philicity. This type of self-organization induces, as is revealed by the nonvanishing behavior of $g_2(r)$ in Figure 4g, Smectic*A*-like orientational order, with the y axes of the particles lying on average normal to the stripes. The long-range fluctuating structure of $g_1(r)$ in Figure 4g is a signature of the antiparallel stacking of successive stripes and of the consequent overall apolarity of the phase.

Finally, at $p^* = 33$, the system undergoes one more first-order phase transition. The final, high-pressure, crystalline phase corresponds to the close packed molecular organization of that system. The molecular rotations are frozen out (see Figure 4h), and the short molecular length dominates the system. This is apparent from the structure of the radial distribution function $g(r)$, which coincides exactly with the corresponding function of a system of hard disks with diameter σ_{min}. To illustrate this, we have plotted on the same graph in Figure 4d the radial distribution function of the system at $p^* = 36$, together with the corresponding function for a system of hard disks with diameter σ_{min} at $p^* = 15$. It is clear that both functions coincide throughout the whole range of distances, indicating an identical type of positional order.

In summary, the $\chi = {}^1/_4$ system exhibits four different phases. Beside the disordered isotropic phase, there are two mesophases with long-range positional order and partial orientational order and a crystalline phase with both positional and orientational order. In the two high-pressure phases, the extended intedigitation of the homophilic molecular sectors causes self-organization into stripes and leads to the formation of channels of the same composition that span the entire simulation box and having widths similar to the coronal thickness.

Turning now the $p^*-\eta$ phase diagram for a system of particles with $\chi = {}^1/_2$, it is apparent from the sharp jump in the density (see Figure 2) that this system exhibits a strong first-order transition at $p^* \approx 22$. Inspection of the snapshots shown in parts a and b of Figure 5 gives a visual impression of the nature of the molecular organization in the two phases. The low-pressure phase is apparently disordered but with the particles tending to form large aggregates. In the peculiar meandering patterns exhibited by the high-pressure phase, the particles form zipper-like stripes that break at irregular distances into orthogonal sections. This orthogonal zigzag produces closed tetragonal loops, spirals, and irregular paths. The paths do not intersect each other, and they end either in themselves, thus forming closed loops, or in a defect, although there are cases where they span the entire simulation box. The latter indicates that the correlation length of these motifs may be longer than the length of the simulation box, and therefore, we are not able to draw strong conclusions regarding the equilibrium pattern of this phase. To investigate the possibility that the formation of such patterns is an artifact of the simulation box size, we have ran a series of simulations with twice the box size. However, the system, in these particular long simulations, showed the same phase behavior and pattern structures with the previous ones. To further investigate the stability of these motifs, we started from perfectly ordered initial conditions, with the particles on a rectangular lattice, forming parallel stripes throughout the simulation box. At very high pressures, the system retains the stripes, but as the pressure decreases, defects gradually start to develop and, well above the

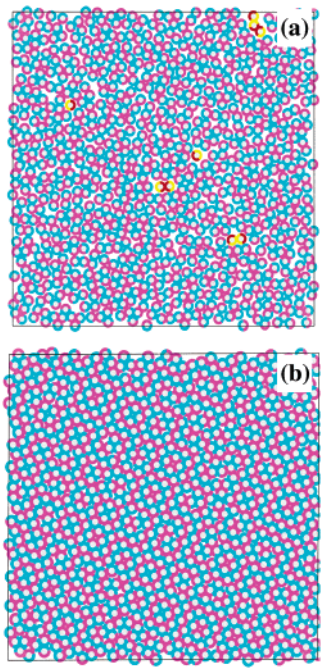

Figure 5. Typical snapshots of the two different phases exhibited by the $\chi = {}^1/_2$ system. (a) Isotropic phase at $p^* = 20$. (b) Crystal phase at $p^* = 30$.

isotropization pressure, the system reverts to the organization obtained upon compression and presented in the snapshot of Figure 5b.

Simulations of systems with even thicker corona, $\chi = {}^3/_4$, reveal new types of molecular organization and pattern formation. Two phases were found upon compression, a disordered isotropic phase that condenses at $p^* \approx 12$, through a rather strong first-order phase transition, to a crystalline phase. Molecular organization in both phases differs substantially from the previously studied phases. Parts a and b of Figure 6 show snapshots at $p^* = 10$ and 15, corresponding to the isotropic and crystal phases, respectively. In the isotropic phase, the particles show a clear tendency to self-assemble in chains that resemble a polymer network. The large corona thickness makes it possible for the homophilic coronal parts of more than two particles to overlap simultaneously. This allows for intersections and branching of molecular chains, thus leading to formation of a large variety of linear, branched, and closed chain configurations. This "global polymerization" breaks down only at very low pressures, well below the crystallization pressure. The disordered nature of this phase is verified by the isotropic radial distribution function, shown in Figure 7a, from which it is clear that positional pair correlations vanish rapidly in contrast to the corresponding correlations in the high-pressure phase (Figure 7b). As in the cases of the previously studied systems, the first two peaks of $g(r)$ are connected to the characteristic interaction lengths. However, a comparison of $g(r)$ with $g_1(r)$, shown in parts a and c of Figure 7, indicates that the orientational correlations extend to appreciable larger interparticle separations as $g_1(r)$ levels off only after interparticle separations of several molecular diameters. Furthermore, the sign alternation, together with the almost constant period between successive peaks of $g_1(r)$, reveals the tendency of the particles to form chains.

Turning now to the high-pressure phase patterns of the $\chi = {}^3/_4$ system, we observe first that triplets of particles self-assemble into aggregates with the hard cores forming the three apexes of an equilateral triangle and with the coronal sectors of the same philicity pointing to the interior of the triangle (see Figure 6c).

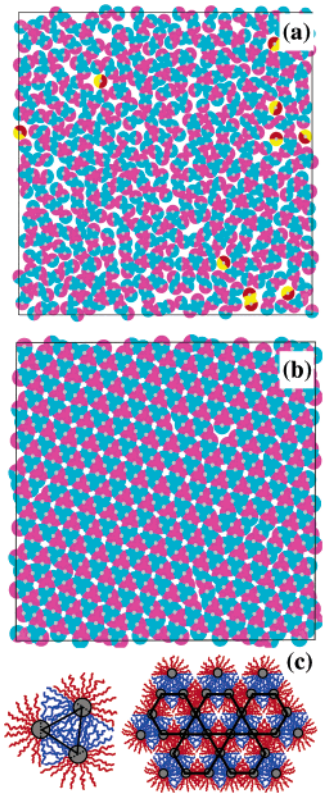

Figure 6. Typical snapshots of the low (a) and high (b) pressure phases exhibited by the $\chi = {}^3/_4$ system taken at $p^* = 8$ and 20, respectively. (c) Schematic representation of a three-particle aggregate (left) and its supramolecular organization in a Kagome lattice (right).

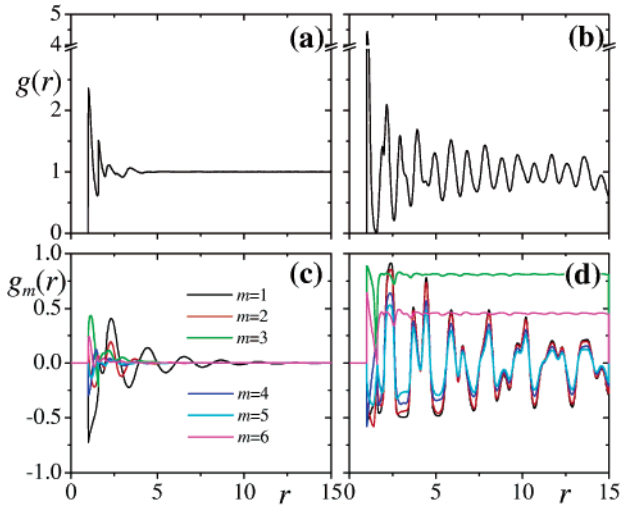

Figure 7. Calculated radial correlation functions (a and b) and orientational correlation functions (c and d) of the two phases exhibited by the $\chi = {}^3/_4$ system at $p^* = 10$ (a and c) and at $p^* = 15$ (b and d).

It is worth noting that this type of self-assembly is suggested for solutions of Janus micelles containing a polybutadiene core with polystyrene and polymethacrylic acid hemispheres.[21] These superparticles, in turn, self-organize into a superstructure with the internal hard cores located on a Kagome-like lattice (see parts b and c of Figure 6). The almost distance-independence long-range behavior of $g_3(r)$ and $g_6(r)$, shown in Figure 7d, is the signature of long-range orientational order with a 3-fold symmetry axis. In addition, the long-range character of the orientational order is confirmed by the fact that the orientational

correlations do not decay with the distance, despite the existence of an appreciable number of defects.

Conclusions

In conclusion, the phase behavior of core−shell Janus particles has been studied by means of Monte Carlo simulations assuming selectively repulsive interactions to mimic the amphiphilicity of the particles. The applied, highly idealized, coarse-grain molecular modeling captures the essential molecular properties of 2D Janus amphiphiles while retaining a minimum number of modeling parameters whose significance is clear. Despite its simplicity, the system exhibits a surprisingly rich phase behavior and by varying the density and/or the amphiphilic shell thickness may produce thermodynamically stable, novel patterns, covering a fascinating variety of topologies. When the internal core is shielded with a very thick corona, extended molecular clustering is obtained, even in the isotropic phase. At high pressures, the system self-organizes into a Kagome-like superstructure, a type of lattice that is of fundamental interest in magnetic systems.[30] Systems with moderately thick coronae exhibit a patterned tetragonal solid phase. Finally, Janus disks with a thin outer shell exhibit a rich polymorphism of crystalline phases. The molecules self-organize on hexagonal lattices with loosely correlated molecular rotations (low pressures) or with nematic-like orientational correlations (moderate pressures) and frozen rotations at high pressures. In view of the ability of the chemist to produce such Janus particles, on the basis of either dendrimers or triblock copolymers or properly coated colloids, this work offers new insights into the molecular functionalization toward the fabrication of precise-patterned surfaces.

Improvements of the present modeling include incorporation of a more realistic, distance-dependent potential for the intercoronal interactions to overcome a clear drawback of the present model according to which overlap of two or more homophilic coronal parts is determined only via geometrical restrictions. Finally, in view of very limited simulation studies on three-dimensional Janus systems,[31] extension of the present model to 3D is in progress.

Acknowledgment. I am grateful to D. J. Photinos and E. T. Samulski for helpful comments on the manuscript. Support through the "Caratheodores" research program of the University of Patras is also acknowledged.

LA052036G

(30) Moulton, B.; Lu, J.; Hajndl, R.; Hariharan, S.; Zaworotko, M. J. *Angew. Chem. Int. Ed.* **2002**, *41*, 2821.

(31) Erdmann, T.; Kroger, M.; Hess, S. *Phys. Rev. E* **2003**, *67*, 041209.